ISSN 2314-5609
Nuclear Sciences Scientific Journal
13, 69-99
2024
https://nssi.journals.ekb.eg

Geology, Petrography and Radioactivity of the Area between Wadi Dib and Wadi Mellaha, North Eastern Desert, Egypt

By

Hossam A. Khamis[1], Darwiesh M. El Kholy[1,] Khairy S. Zaki[2], Mohamed M. Said[1]

[1] **Nuclear Materials Authority**

[2] **Geology Dept. Faculty of Science, Minia University**

ABSTRACT

A varieties of rocks including metavolcanics, metagabbro-diorite complex, older granitoids, Dokhan volcanics, Hammamat sediments, younger granites as well as dyke swarms and veins are well exposed and studied in details at the strip enclosed between Wadi (W) Dib and W. Mellaha area. The metavolcanics is represented by the basic variety of metabasalt, intermediate variety of meta-andesite and acidic varities of meta-dacite and meta-rhyolites in addition to meta- pyroclastics. The metagabbro-diorite complex is shown intruding the metavolcanics and enclave rafts of then while this complex is intruded by both the older and younger granites and mainly have the composition of metamorphosed gabbros. The older granitoids in the area are seen extruded by the Dokhan volcanics and are intruded by the younger granites and generaly have the composition of quartz- diorite and granodiorites.

The Dokhan volcanics in the study area are present and exposed at W. Dib, W. Abu Had and W. Mellaha while they are represented by successive sequences of lava flows ranging in composition from intermediate to acidic varieties with their related pyroclastics. A wide spectrum of different types of molasses rocks is represented by the Hammamat sediments which have conglomerates, greywakies, purple slate and siltstone. The younger granitic rocks which are considered the most important, from the radioactivity point of view, are classified into syenogranite and alkali feldspar granite varieties and are shown intruding all the rock units exposed in the area. Numerous post-granitic dyke swarms and veins are recorded as basic and acidic dykes invading and cutting all the rock types in the study area.

The radioactivity of the investigated rocks show an increase in their values from the older unites to the younger one where the radioactivity is in harmony with the increase of the radioelement content. The younger granitic rocks show the highest values of radioactivity among the other rock units. An anomalous pegmatite body is recorded along a tributary branched from W. Mellaha has 157 ppm uranium content and 4350 ppm thorium content and 4.23 K% and is formed at the pneumatulitic (pegmatite) late stage of the alkali feldspar granites.

WADI DIB AND WADI MELLAHA, NORTH EASTERN DESERT

I. INTRODUCTION

The study area is located in the northern part of the Eastern Desert of Egypt. It is situated in the Red Sea mountain ridges at about 80 km northwest of Hurghada City between latitudes 27º 30' 00" - 27º 45' 00 N and longitudes 32º 50´ 00˝ - 33° 10' 00" E (Fig. 1). It covers an area of about 700 Km² and is mainly covered by Neoproterozoic basement rocks of a relatively rough mountainous topography such as G. Subir (or Zubir) (1398 m.a.s.l.), G. Melaha (1119 m.a.s.l.) , G. Abu Had (763 m.a.s.l.) , and G. Ladid al-ji`dan (1113 m.a.s.l.) and the area is accessible through wadies that drain toward the Red Sea coast which are W. Dib , W. Abu Had, W. Ladid al ji`dan and W. Melaha While W. Um Sitw is a southern branch of W. Dib (Fig. 2).

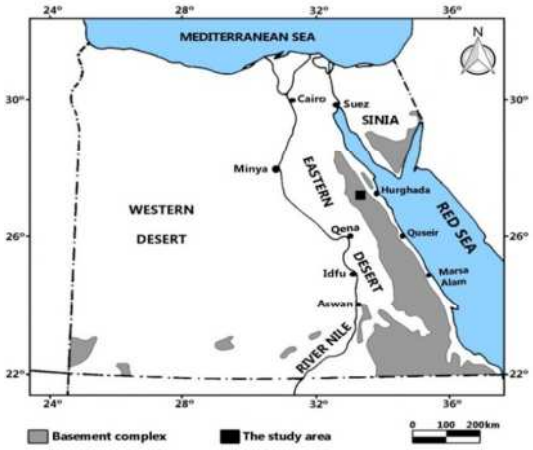

Fig. 1: Location map of the studied area, North Eastern Desert, Egypt

Remarkable differences in the lithology and structural patterns of the exposed ED basement made Stern and Hedge (1985) and El-Gaby et al. (1988) to subdivide ED into three tectonic provinces: North Eastern Desert (NED), Central Eastern Desert (CED), and South Eastern Desert (SED). The NED province comprises a number of granitic intrusions with some exposures of island arc metavolcanics, metasediments, Dokhan volcanics and Hammamat Molasse sediments.

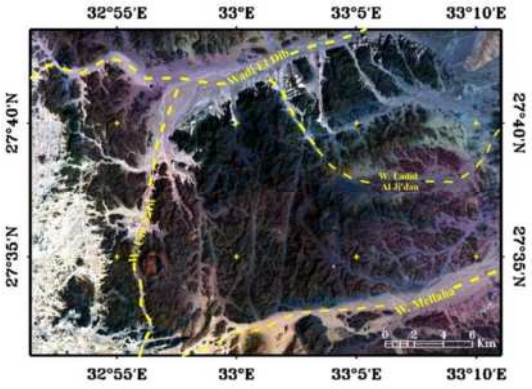

Fig. 2: Landsat image (TM) of the study area showing main wadies

Many authors have been worked in the area in mapping, field description of the different rock units as well as the petrogenisses and tectonic evoluation of the area. These works include Francis (1971), Francis (1972), El Ramly et al. (1976) and Masoud et al. (1998) for mapping the different rock types in the area and environs and its structure evolution. Garson and Krs (1976), Sabet et al. (1977), Serencsits et al. (1979), El Sheshtawi et al. (1995), Hassanen et al. (1997) and Ghoneim et al. (1999) were interested in studying the ring complex of W. Dib and its evolution and different units constituting it. Mussa and Dardier (1982), Ressetar and Monrad (1983), Ahmed (1983), Heikal and Ahmed (1984), Heikal and Ahmed (1983), Ries et al. (1983) and Ragab (1987) were shed lights on the evolution of the Dokhan Volcanics in the area around G. Abu Had and its different lava flows and pyroclastics as well as the associated Hammamat Sediments. Rabie et al. (1994), Rabie et al. (1996), Hamoudah (1998), Ali (2001), Ahmed and Ali

(2003), Ayoub (2003) and Hammad (2005) were caring about the younger granitic rocks from their geochemistry, petrography, radioactivity and hydrothermal activity points of view.

II. GEOLOGICAL SETTING

A geological map at scale 1: 40,000 was prepared for the studied area (Fig. 3). According to the field relationships, the rock types exposed in the studied area can be arranged in the following geologic sequence according to the classification of the basement rocks of Egypt by **El Ramly (1972)**:

Dykes and Veins … (youngest).
Younger Granites
Hammamat Sedimentary Rocks
Dokhan Volcanics
Older Granitoids
Metagabbros-diorite complex
Metavolcanics…….. (oldest).

II.1 METAVOLCANICS

The metavolcanics and related metavolcaniclastic sediments represent the oldest rocks of the studied area and are recorded in different localities forming highly weathered hills of low topography (Fig. 4). They are intruded by the older granites which carry them as roof-pendant (Fig. 5). These metamorphosed rocks are partially to completely altered due to secondary processes where the most common alteration features are chloritization and epidotization (Fig. 6).

In some localities the metapyroclastics show different grain sizes up to pebble size (Fig. 7).These pebbles are sometimes found as rounded to sub rounded clastics which solidified together forming the meta agglomerate (Fig. 8). It is important to state that the foliation is very clear in the metavolcanics (Fig. 9). In some localities, several dykes and Quartz veins are cutting the metavolcanics (Figs. 10 and 11).

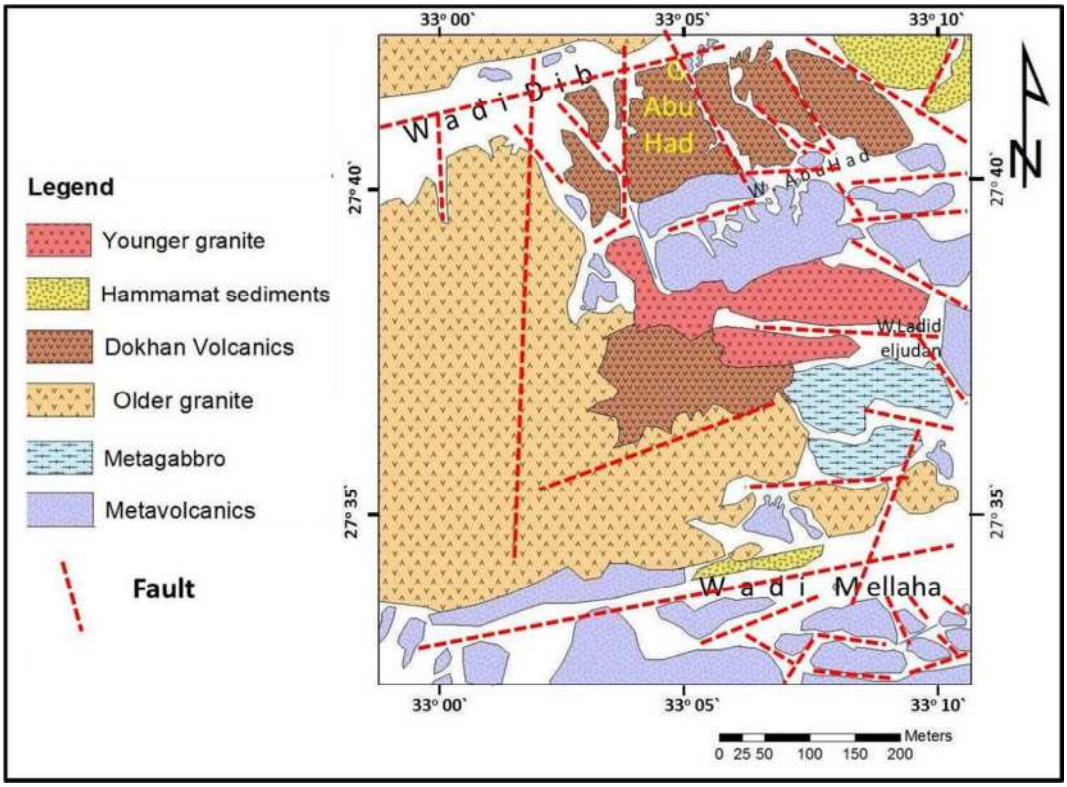

Fig. 3: The Geological Map of the Area between W. El Dib and W. Mellaha

Fig. 4: shows low topography of metavolcanics.

Fig. 5: shows the contact between older granite and metavolcanics

Fig. 6: shows epidotization in the Metavolcanics.

Fig. 7: shows pebble-sized grain in the Metavolcanics.

Fig. 8: displays the meta agglomerates.

Fig. 9: displays the foliation in the Metavolcanics

Fig. 10: shows an acidic dyke cutting the Metavolcanics

Fig. 11: shows Quartz vein in the Metavolcanics.

According to the field observations, these rocks can be recognized as basic, intermediate and acidic metavolcanics as well as related metavolcanoclastics and both are intercalated with each other. The fine grained and massive basic metavolcanics are essentially of basaltic composition and they are dark grey in color. The intermediate metavolcanics mainly consist of meta-andesites which sometimes exhibit porphyritic texture. The acidic metavolcanics are mainly fine grained massive rocks that represented by metadacites, metarhyolites which are of grey to pale brown in color respectively. The acidic metavolcanics are associated with the intermediate

metavolcanics and interfingered with acidic metavolcanoclastics in repeated cycles with a distinctive foliations.

II.2 METAGABBRO-DIORITE COMPLEX

The rocks of the metagabbro represent a major rock unit among the basement complex of Egypt, however several classifications were suggested for the Egyptian gabbroic rocks. **Abu El-Ela (1985)** stated that the metagabbro of the Eastern Desert of Egypt may be subdivided into ophiolitic metagabbro and metagabbro of island arc.

In the study area, the metagabbros are related to those of the Island Arc type and commonly called metagabbro-diorite complex. These rocks are well exhibited as small isolated and scattered hills at W. Ladid Al Jui'dan and to the south-east of W. Ladid al Ji'dan. They are pale to dark grey in colour, medium to coarse grained, massive and generaly weathered to spheroidal boulders (Figs. 12 and 13).These rocks intrude the metavolcanics and took xenoliths of different shapes and sizes from them. On the other hand they are intruded by the older granitoids and younger granites which send several offshoots into them. The thickness and intensity of these offshoots decrease gradually away from the contact. The microfractures of these rocks are sometimes filled with quartz and feldspar veinlets.

Fig. 12: shows massive, weathered gabbroic rocks;

Fig. 13: shows spheroidal gabbroic rocks.

II.3 OLDER GRANITOIDS

Older granitoids are named as grey granites (**Hume, 1935; El Ramly and Akaad, 1960**), synorogenic plutonites (**El Shazly, 1964**), older granites (**Akaad and Noweir, 1969; El Ramly, 1972**), syn to late tectonic plutonites (**El Ramly, 1972**), syntectonic and GI grey granites (**Hussein et al., 1982**), subduction-related arc granitoids (**Takla, 2002**) and as calc-alkaline granite series (**El Gaby, 2005**).

The older granitoids in the study area are well exposed at W. Milaha, and the western part of the area. They are characterized by low to moderate topography, exfoliation and bouldery weathering with characteristic huge bloocks (Fig. 14).

Generally, the older granitoids are represented by the quartz diorite and have grey to pale pink colour, medium to coarse grained and show marked variation in their composition. In some stations, the frequent presence of relics of metavolcanics as xenoliths is a characteristic feature in these rocks (Fig. 15). On the other hand the older granitoids are invaded by the dokhan volcanics and are intruded by the younger granites (Figs.16 and 17).

In some localities, the older granites are invaded by composite dyke which form from both acidic and basic composition in the same location (Fig. 18). In other localities, the older granite is overlain by the metavolcanics as a roof pendant which is resting on them (Fig. 19).

Fig. 14: shows moderate topography, and bouldery weathering

Fig. 15: shows xenolithes of Metavolcanics in older granites

Fig. 16: displays the relation between both older and younger granites

Fig. 17: displays the relation between older granite and Dokhan volcanics

Fig. 18: shows a composite dyke in the older granite.

Fig. 19: shows the relation between the metavolcanics and older granite.

II.4. DOKHAN VOLCANICS

The Dokhan volcanics in the studied area are present at W. Dib ,W. Abu Had and W. Milaha. Generally, they are of moderate relief, very fine grained and grey to greyish pink in colour. The Dokhan volcanics are extrude in the metavolcanics, metagabbros and older granitoids On the other hand, they are intruded by the younger granites which took xenoliths of various shapes and sizes from them. The contact between the Dokhan volcanics and the metavolcanics is not clear due to the similarity of colour between them while the contact with the other rocks is sharp (Figs. 20 and 21). **El Gaby (1983) and El Gaby et al. (1984 and 1988)** believe that the Dokhan volcanics and Hammamat sedimentary rocks are penecontemporaneous.

The Dokhan volcanics are represented by successive sequences of lava flows ranging in composition from intermediate to acidic varieties with their related pyroclastics. The lava flows are

affected by low grade metamorphism and alteration processes. The main alteration processes are chloritization and epidotization (Fig. 22). The pyroclastics are predominant than lava flows and are found associated with them. They are highly compact, hard, massive and represented by lapilli tuffs (Fig. 23).

Fig. 20: displays sharp contact between Younger granites and Dokhan volcanics

Fig. 21: displays the relation between Dokhan volcanics and Metavolcanics.

Fig. 22: shows epidotization in Dokhan volcanics.

Fig. 23: shows lappili tuffs in Dokhan volcanics.

II.5 HAMMAMAT SEDIMENTS

The Hammamat sedimentary rocks in the studied area are exposed at both sides of W. Dib and at the northern side of W. Milaha as scattered masses of low to moderate topography. They are intruded by younger granites and locally intermixing with lava flows of Dokhan volcanics at the base of their sequences, which may be contemporaneous with the deposition of the basal parts of these sediments. They are slightly metamorphosed and have different colours of light grey, greenish grey, deep green and black (Figs. 24 and 25).

Generally these rocks are poorly sorted, compositionally and texturally immature due to their deposition in situ or by a very short distance of transportation and rapid rate of deposition as thick piles in deep basins. They are intercalated with Dokhan volcanics. In some cases these rocks are altered.

The conglomerates are poorly sorted, polymictic, massive and contain rounded to sub-rounded pebbles and cobbles of various rock types, cemented by fine matrix of greyish-green materials. These pebbles and cobbles are provided from the older rocks such as metavolcanics, metagabbros, Dokhan volcanics, older granitoids and reworked fine-grained Hammamat sedimentary rocks. They were subjected to different degrees of deformation as indicated by the development of schistosity in the matrix and elongation, flattening as well as the stretching of the pebbles. The conglomerate beds are ranging in colour from within the conglomerates and greywacke beds. They are grey in colour, fine grained and sometimes

exhibit laminations and foliations. The microfractures dark green to greyish-green depending on the type of rock fragments, composition of the matrix and alteration effects (Fig. 26). The slates are less common and occur as intercalations of these rocks are sometimes filled with quartz and feldspar veinlets (Fig. 27).

The greywackes have grey and greyish green colours depending on their compositions, source rocks and alteration effects. They are massive to slightly foliated, jointed and are intercalated with conglomerate beds. Some of the greywackes are pebbly, in which the grain size is ranging from 1 mm to 5 mm. They usually show graded bedding ranging from pebbly size grading upward to fine grain size (Fig. 28). In some localities, it is found that the younger granite is overlain by the Hammamat sediments with sharp contact as shown in (Fig. 29); this interpreted as they carried them during the ascending process.

Fig. 24: shows the topography of the Hammamat Sediments comparing to the Younger granites.

Fig. 25: shows the contact between the Hammamat Sediments and the Younger granites.

Fig. 26: shows the coarse grained conglomerate.

Fig. 27: shows the fine grained slate.

Fig. 28: shows the fining upward sequence of conglomerate and grywakes.

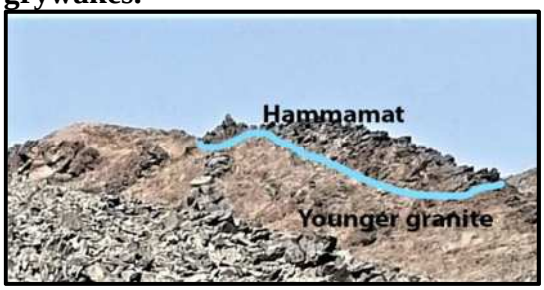

Fig. 29: shows the intrusive contact between Hammamat sediments and younger granites.

II.6. YOUNGER GRANITE

The younger granites of the studied area are exposed in the area between W. Abu Had and wadi Ladid Al-jui'dan. The studied younger granites are relatively of limited distribution and represented by elongate curved, high

relief masses present to the south of W. Abu Had.

These granites are the youngest among all the described rock units in the studied area. They intrude the older pre-existing rock units with typical sharp intrusive contacts (Fig. 30).

Generally, the younger granites are distinguished by their red to pink colours, massive appearance and by the absence of foliation but exfoliation and jointing are present (Fig. 31). Moreover, the marginal granitic parts are commonly fine grained exhibiting a notable amount of mafic minerals.

These rocks are altered in some parts due to secondary processes. The most common alteration features are hematitization, epidotization, chloritization and kaolinitization, especially, along joint planes (Fig. 32).

In most localities; the studied younger granites are represented by blocky-shaped masses with high topography and relatively high resistance to weathering and erosion. (Fig. 33).

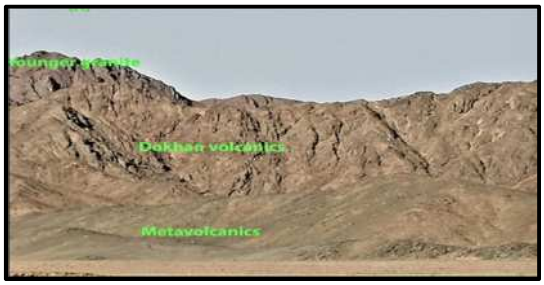

Fig. 30: General view showing the relation between the younger granite and the pre-existing rock units.

Fig. 31: shows the pink, exfoliated and jointed coarse-grained granites.

Fig. 32: shows the alteration along joint surface in the younger granites.

Fig. 33: General view of younger granites exposures

II.7. PEGMATITES

Pegmatites in the study area are granitic in composition. They are very coarse grained and occur as irregular forms and pockets. Some pegmatitic bodies at W. Ladid al-Ji' adan are associated with the younger granites. They are pink to pinkish white in colour and consist mainly of quartz and potash feldspar and some muscovite (Fig. 34).

Fig. 34: shows the pegmatitic body in the younger granites.

II.8: POST GRANITE DYKES:

All the basement rocks of the NED are dissected by systems of dyke swarms which represent the youngest rock type ranging in age from 589 - 543 Ma (Stern and Hedge, 1985).

In the study area, these dykes are penetrated and cut all the previously described rock types. They range in thickness from 0.5 m to10 m and extend for several kilometers in length. They run parallel to each other in swarms striking NE-SW to ENE-WSW.

They are arranged from oldest to youngest to three groups:

Acidic, intermediate and basic dykes depending on their crosscutting relations (Hassan and Hashad, 1990).

2.8.1. ACIDIC DYKES

In the study area, acidic dykes are mainly represented by granite porphyry, granophyres, rhyolite and dacite dykes. They are generally fine grained, massive, fresh and hard displaying different shapes and various colours including red, reddish pink, buff to pale brown colours and more resistant to erosion than the enclosing rocks forming prominent spines and ridges. They are characterized by their sharp straight contacts with more or less vertical slopes. These dykes follow ENE-WSW direction. Some of them are rejuvenated by magma intrusion forming huge dykes (Figs.35, 36 and 37).

Fig. 35: shows acidic dyke in Metavolcanics.

Fig. 36: shows acidic dyke in Dokhan volcanics.

Fig. 37: shows acidic dyke in Older granite.

2.8.2 BASIC DYKES

These dykes are the youngest in the study area cutting all the previously studied rock types following NE-SW trend. They are distributed all over the area especially in the younger granites. They are hard, massive, straight to slightly curved, of long extensions, ranging in the thickness from few centimeters to more than 3 m, displaying various shapes and sometimes grouped together to form dense dyke swarms. They are deeply weathered than their host rocks and occasionally form deep elongated trenches and grooves especially when they intrude the younger granites (Figs. 38, 39 and 40). They are highly affected by faults.

They are represented by dolerite and basalt. Dolerite dykes are medium grained and greenish grey to dark grey in colour, while basalt dykes are fine grained and dark greenish grey to black in colour.

Fig. 38: shows Doleritic basic dyke.

Fig. 39: shows basic dyke in Older granite.

Fig. 40: shows basic dyke in Younger granite.

III. PETROGRAPHY

Representative rock samples from the exposed different rock types were collected, then, Forty-Three thin sections were prepared to study the mineralogical and textural characteristics of the different rock types by using the polarizing microscope.

3.1.METAVOLCANICS.

According to field and petrographic studies, Metavolcanics can be classified to basic, intermediate and acidic varieties as well as their metavolcanoclastics. The basic metavolcanics are mainly dominated by metabasalts, the intermediate by meta-andesites while the acidic metavolcanics are mainly represented by metadacites and metarhyolites.

3.1.1.METABASALTS

Based on the textural variations, metabasalts in the study area are essentially composed of plagioclase, clinopyroxene and olivine phenocrysts embedded in fine-grained groundmass to show the porphyritic texture. Opaques are the dominant accessory minerals while epidote and zoisite occur as secondary minerals (Figs.41, 42, 43 and 44).

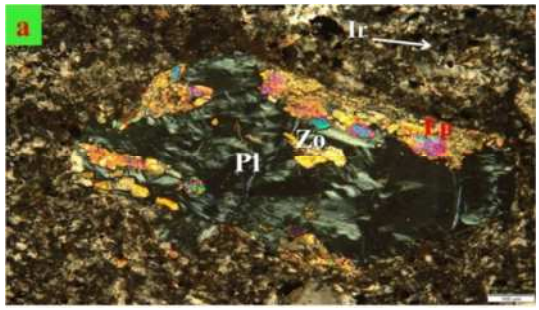

Fig. 41: Plagioclase (Pl) altered to zoisite (Zo) and epidote (Ep) with scattered iron oxides (Ir) in metabasalt.

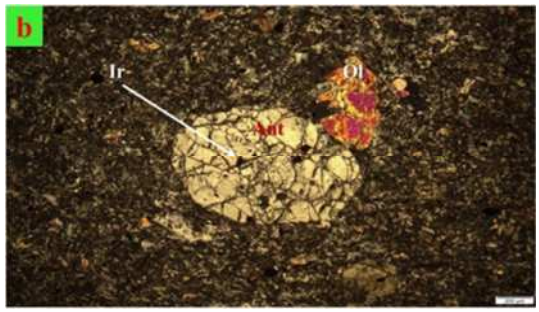

Fig. 42: Phenocrysts of olivine (Ol) and antigorite (Ant); (Pseudo morph of olivine (Ol); with inclusions ofiron oxides (Ir) in metabasalt.

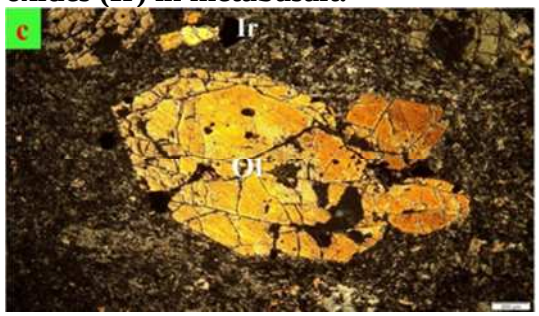

Fig. 43: Pseudo morphous olivine (Ol) altered to actinolite and corroded by the groundmass in metabasalt.

Fig. 44: Phenocrysts of olivine (Ol) and pyroxene (Px) in metabasalt.

3.1.2 META-ANDESITES

The meta-andesites are hard, massive, fine grained and porphyritic rocks. They are dark greyish green in color.

Microscopically, meta-andesites are commonly porphyritic and composed of plagioclase and hornblende phenocrysts embedded in fine-grained groundmass. Opaques are the main accessory minerals while chlorite, epidote and saussurite occur as secondary minerals. Sometimes, this rock type is fractured; some of these fractures are filled with secondary muscovite (Figs. 45, 46, 47and 48).

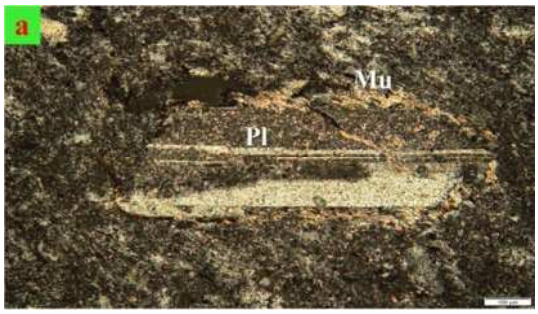

Fig. 45: Phenocryst of plagioclase (Pl) corroded by the muscovite (Mu) and shows the porphyritic texture in metaandesite.

Fig. 46: Small laths of plagioclase (Pl) occupying the groundmass in metaandesite.

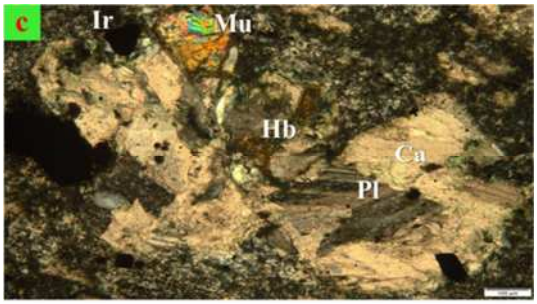

Fig. 47: Glomeroporphyritic texture (clusters of plagioclase (Pl), hornblende (Hb), muscovite (Mu) and calcite (Ca)) in metaandesite.

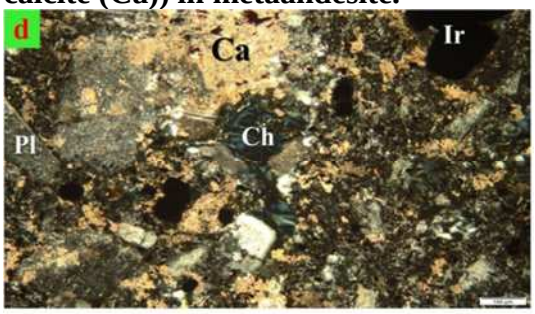

Fig. 48: Chloritization (Ch) and carbonitization (Ca) of plagioclase (Pl) crystals with anhedral crystal of iron oxides (Ir) in metaandesite.

3.1.3 METADACITES

Metadacites are of limited distribution in the study area. They are commonly porphyritic and composed of quartz, plagioclase and biotite as well as subordinate amount of potash feldspars embedded in a cryptocrystalline groundmass formed of small lathes of plagioclase, quartz, biotite, epidote and chlorite. Zircon and iron oxides are found as accessory minerals (Figs. 49 and 50).

Fig. 49: Subhedral crystals of plagioclase(PL)and quartz(Q) in equigranular textured metadacite.

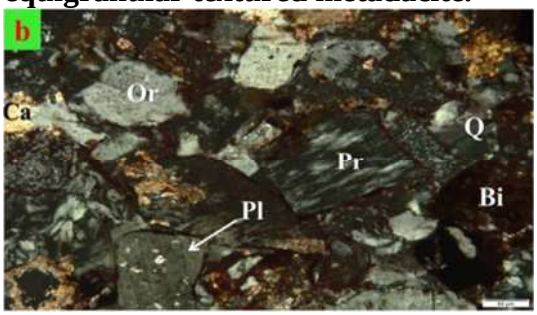

Fig. 50: Subhedral crystals of plagioclase(PL), quartz(Q)and string perthite(Pr) in metadacite.

3.1.4 METARHYOLITES

Metarhyolite is less dominant than metadacite in the area of study. It is composed essentially of potash feldspar, quartz and plagioclase phenocrysts ranging in size from 0.3 to 1.6 mm across embedded in a fine-grained groundmass composed of quartz, muscovite and feldspar minerals. Zircon and iron oxides occur as accessory minerals. The porphyritic and spherulitic textures are more common in this rock (Figs.51 and 52).

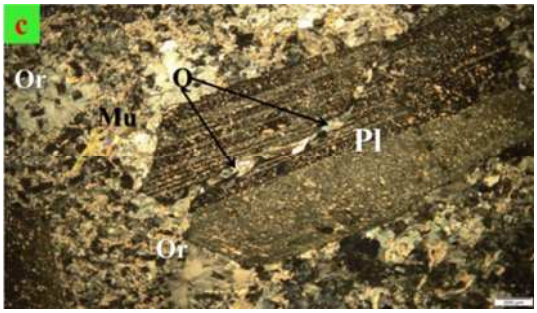

Fig. 51: Phenocryst of fractured,sericitized plagioclase(Pl) in metarhyolite.

Fig. 52: Phenocryst of quartz(Q) in metarhyolite.

3.2.METAGABBRO.

Metagabbros are medium to coarse grained rocks, equigranular and mainly composed of hornblende and plagioclase with subordinate amount of pyroxene. The main accessory minerals are iron oxides, cassiterite and titanite while epidote, actinolite and antigorite are found as secondary minerals (Figs. 53 , 54 , 55 , 56).

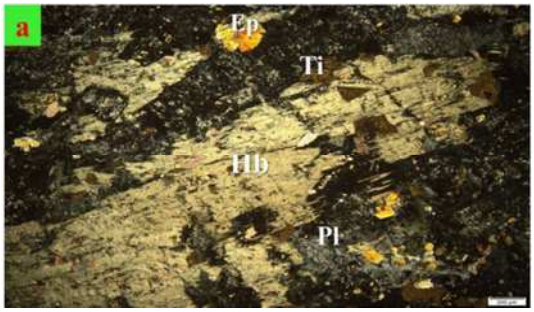

Fig. 53: Phenocryst of hornblende (Hb) corroded by the plagioclase (Pl) and surrounded by the titanite (Ti) in the metagabbro.

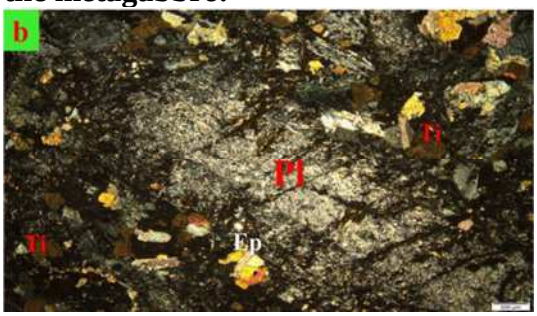

Fig. 54: Phenocryst of saussuritized plagioclase (Pl) surrounded by epidote (Ep) and titanite (Ti) in the metagabbro.

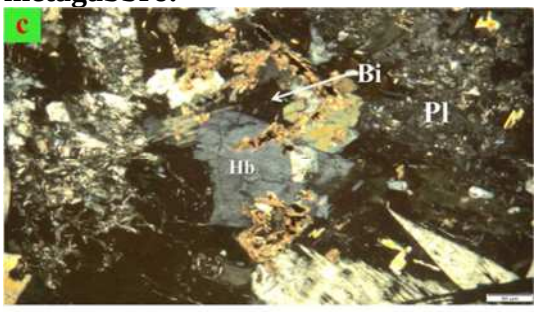

Fig. 55: The biotite (Bi) is corroded by the hornblende (Hb) and plagioclase (Pl) in the metagabbro

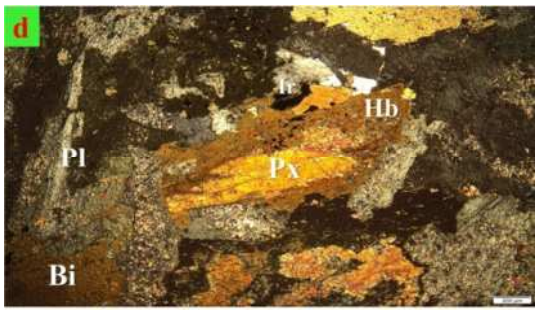

Fig. 56: Incomplete corona between hornblende (Hb) and pyroxene (Px) in the metagabbro.

3.3. OLDER GRANITOIDS

The older granitoids are medium to coarse grained, hypidiomorphic and equigranular rocks. Q-A-P triangle (Streckeisen, 1976) is used for the nomenclature of older granitoids. In the present work, eight thin sections were chosen for modal analysis (table 1). According to the modal classification of Streckeisen (1976), quartz, plagioclase and potash feldspars were recalculated to 100% and plotted in Q-A-P diagram. The older granitoids were plotted within the granodiorite and quartz diorite fields (Fig. 57). Quartz diorites are characterized by low abundance of potash feldspars relative to granodiorites.

These rocks are composed of plagioclase, quartz, potash feldspars, biotite as essential minerals. Zircon, iron oxides and sphene are present as accessory minerals while chlorite and epidote as secondary minerals (Figs. From 58 to 65).

Table (1): The modal analyses of the studied older granitoids of the study area.

S. No.	Mineral composition						
	Quartz (Q)	K-feldspar (A)	Plagioclase (P)	Biotite	Muscovite	Accessories and opaques	Total
44	10.15	5.60	72.30	4.10	3.60	4.25	100%
43	11.19	4.11	73.22	3.55	3.45	4.48	100%
42	12.25	5.21	71.61	3.13	3.77	4.03	100%
41	13.38	3.98	68.09	4.54	4.67	5.34	100%
40	21.53	14.31	47.88	3.07	7.35	5.86	100%
39	23.32	13.20	48.21	2.96	6.88	5.43	100%
38	25.56	14.19	45.34	3.10	5.89	6.01	100%
37	26.55	15.76	42.29	4.08	6.82	4.50	100%

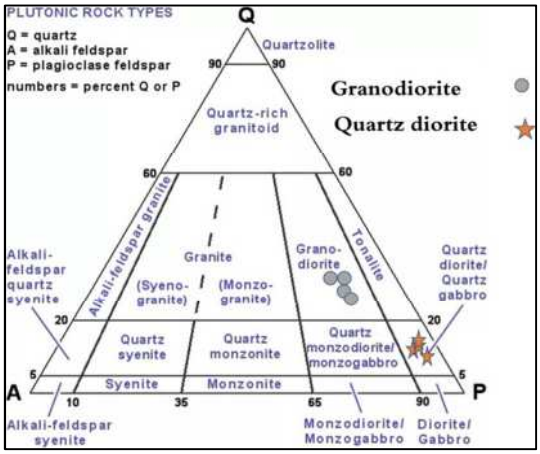

Fig. 57: Ternary diagram (Streckeisen, 1976) for modal quartz (Q), alkali feldspar (A) and plagioclase (P) of the studied older granitoids.

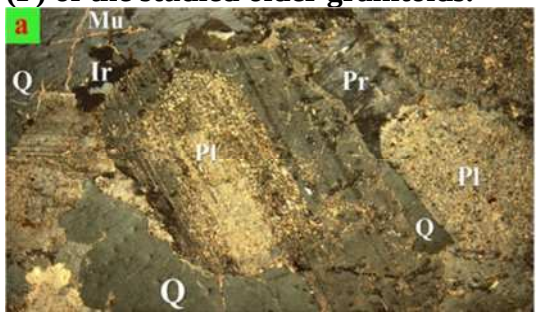

Fig. 58: Saussuritized plagioclase (Pl) corroded by quartz (Q), perthite (Pr) and iron oxides (Ir) in granodiorite

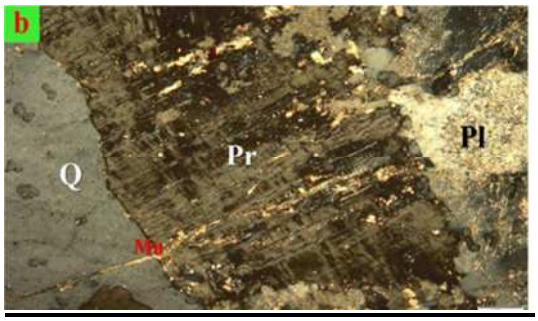

Fig. 59: Fractured perthite (Pr) filled with muscovite (Mu) and corroded by quartz (Q) and plagioclase (Pl) in granodiorite.

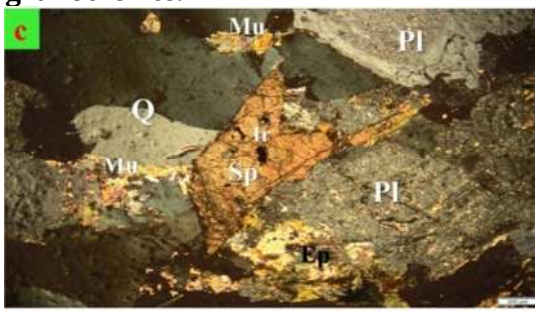

Fig. 60: Sphene (Sp) is corroded by the plagioclase (Pl) and quartz (Q) and has small inclusions from the iron oxides (Ir) in quartz diorite.

Fig. 61: Sphene (sp) surrounded by altered plagioclase (Pl) in granodiorite.

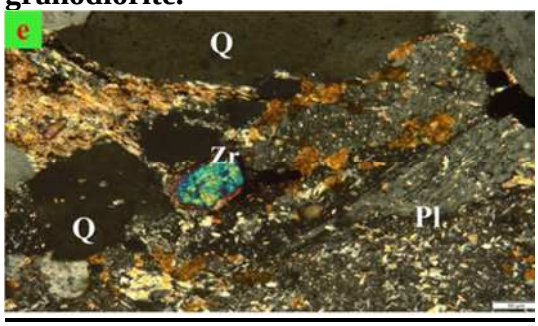

Fig. 62: Zircon (Zr) in the altered plagioclase (Pl) crystals as inclusions in granodiorite.

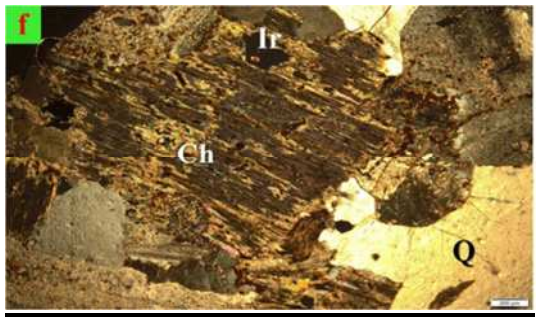

Fig. 63:Chlorite (Ch) containing iron oxide (Ir) as inclusions and is corroded by quartz (Q) in granodiorite.

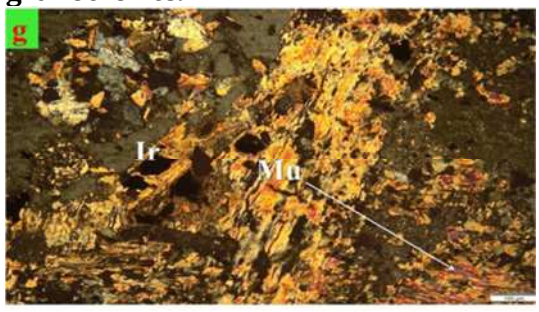

Fig. 64:Muscovite (Mu) encloses several inclusions of iron oxide (Ir) in quartz diorite.

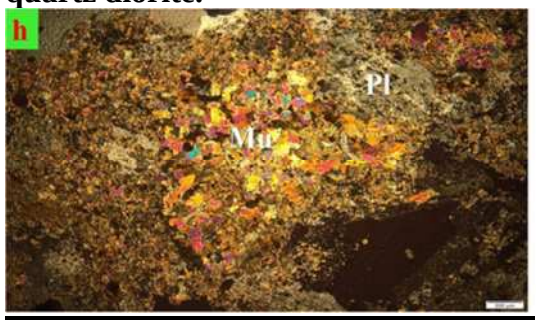

Fig. 65: Aggregates of muscovite (Mu) corrode the plagioclase crystal (Pl) in quartz diorite

3.4 DOKHAN VOLCANICS

According to field and petrographic studies, dokhan volcanics are represented by tuff and agglomerate pyroclastics. The tuffeous pyroclastics are divided into lithic, lithic crystal and crystal tuffs, while agglomeratic pyroclastics include lithic and lithic crystal agglomerates.

3.4.1. TUFFS

3.4.1.1. LITHIC TUFFS

These rocks are massive, fine grained and ranging in colour from greyish white to grey having greenish white colour in case of alteration. Microscopically, they are represented by andesitic lithic tuffs. The lithic fragments are andesitic, basaltic and sometimes are basaltic andesite in composition. Andesitic lithic fragments consist of plagioclase and mafics of chloritized hornblende, whereas the basaltic lithic fragments consist of plagioclase, hornblende and pyroxene minerals. These lithic fragments are corroded and embedded in a fine grained tuffaceous groundmass of andesitic composition (Figs.66, 67 and 68).

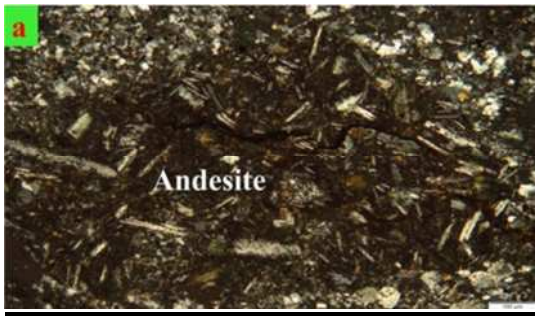

Fig. 66: Lithic fragments of the andesite in lithic tuff.

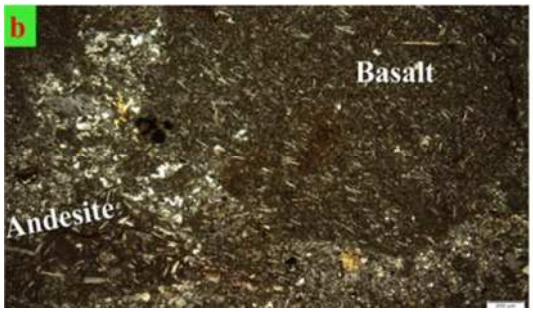

Fig. 67 : Lithic fragments of the basalt and andesite in lithic tuff.

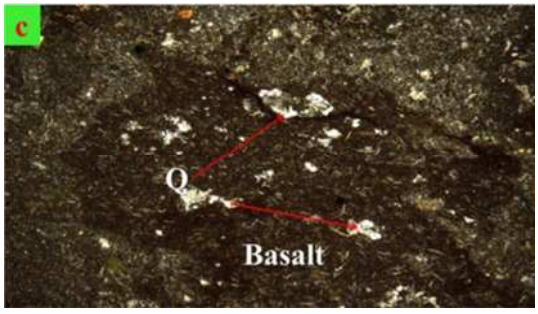

Fig. 68: Amygdoidal lithic fragments of the basalt in lithic tuff.

3.4.1.2. CRYSTAL TUF

They are massive, fine to medium grained and range from reddish grey to grey in colour. Microscopically, they consist of abundant crystals of plagioclase, quartz, biotite, hornblende and iron oxides (Fig. 69).

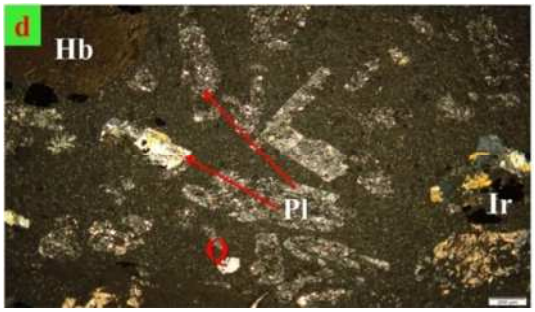

Fig. 69: Crystal fragments of the plagioclase (Pl), hornblende (Hb), quartz (Q) and iron oxides (Ir) in crystal tuff.

3.4.1.3. LITHIC CRYSTAL TUFFS

These rocks are medium grained and consist of both crystal and lithic fragments. The crystal frgments are represnted by plagioclase and muscovite, whereas the lithic fragments are of andesitic and basaltic composition. Andesitic lithic fragments consist of plagioclase, quartz and mafic minerals. The basaltic fragments are composed of plagioclase and biotite set in a fine grained groundmass of the same constituents. These rocks are strongly welded and contain welded glass fragments of ash size (Fig. 70 and 71).

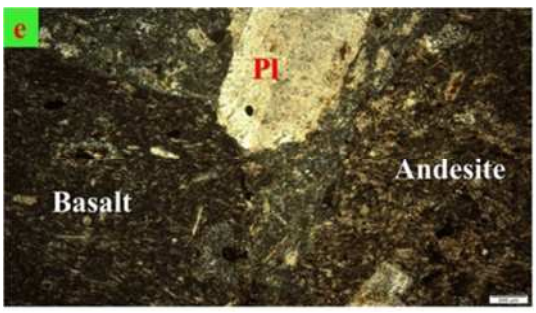

Fig. 70: Lithic fragments of the basalt and andesite and crystal fragments of the plagioclase (Pl) in lithic crystal tuff.

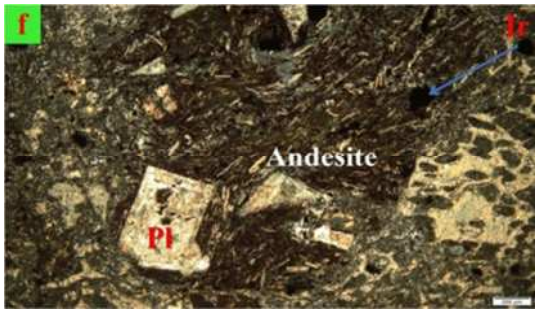

Fig. 71: Crystal fragments of the iron oxides (Ir) and plagioclase (Pl) with lithic fragments of the andesite in lithic crystal tuff.

3.4.2. AGGLOMERATES

3.4.2.1. LITHIC CRYSTAL AGGLOMERATES

They are compact, poorly sorted, coarse grained and grey in colour. Microscopically, these rocks are mainly composed of angular fragments of porphyritic andesite and basalt as well as plagioclase, biotite and iron oxide crystals embedded in a fine grained groundmass. Porphyritic andesite and basalt are highly compacted and commonly cemented by very fine dark grey tuffs.

The fine grained matrix occurs in very thin screen filling the interstitial spaces between the rock fragments. Chlorite, sericite and epidote are found in the cement or associated with andesite as alteration products (Figs.72 and 73).

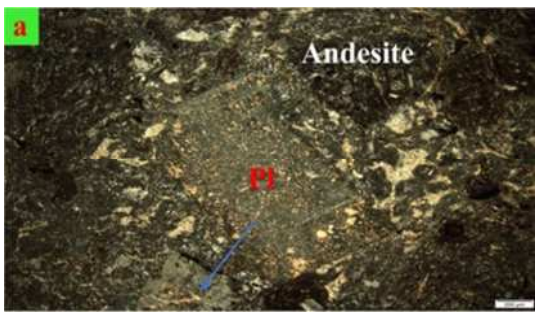

Fig. 72: Lithic fragments of the andesite and crystal fragments of plagioclase (Pl) in lithic crystal agglomerates.

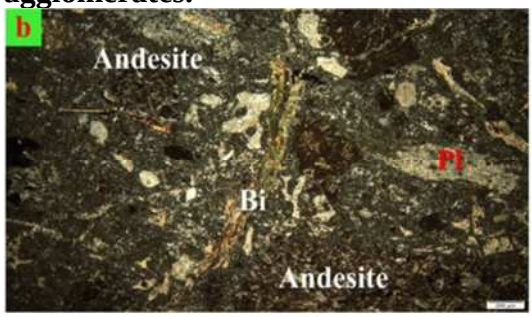

Fig. 73: Crystal fragments of the biotite (Bi) and plagioclase (Pl) with several lithic fragments of andesite in lithic crystal agglomerates.

3.4.2.2. CRYSTAL AGGLOMERATES

Microscopically, these rocks are mainly composed of euhedral to subhedral crystals of altered plagioclase and hornblende embedded in a fine grained tuffeous groundmass composed of tiny crystals of plagioclase, actinolite, chlorite and iron oxides.

Plagioclase (An_{18-23}) occurs as euhedral to subhedral long prismatic phenocrysts. It mainly contains oligoclase and some albite. It is altered to sericite and epidote and contains inclusions of iron oxides.

Hornblende occurs in two generations. The first generation is xenomorphic crystals enclosing relics of iron oxides. The second generation occurs as subhedral to euhedral crystals. Occasionally, the hornblende crystals of the second generation are altered to pale yellow actinolite and bluish green chlorite (Figs. 74 and 75).

Fig. 74: Crystal fragments of altered hornblende (Hb) and plagioclase (Pl) with iron oxide inclusions in crystal agglomerates.

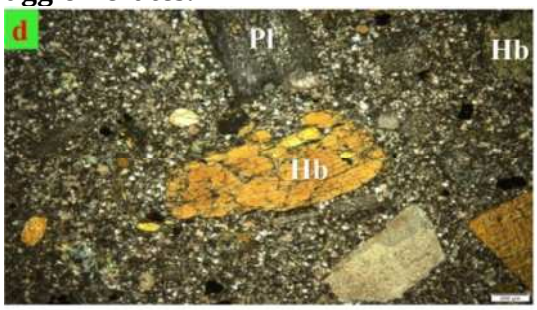

Fig. 75: Crystal fragments of altered hornblende (Hb) and plagioclase (Pl) with iron oxide inclusions in crystal agglomerates.

3.5 HAMMAMAT SEDIMENTARY ROCKS

Conglomerates and greywackes mainly represent the Hammamat sedimentary rocks at the studied area while siltstones are of limited distribution. In hand specimens, the Hammamat sedimentary rocks are mainly of green to dark grey colors. Some varieties show reddish tint. All Hammamat varieties are ill sorted, but the siltstones are rather sorted than the greywackes.

3.5.1 CONGLOMERATES

Conglomerates are polymictic constituting stretched, sub-rounded pebbly-size rock fragments, usually oriented in definite directions indicating that they were subjected to stress. The spherical pebbles are very rare. The pebbles are mainly represented by metavolcanics (metarhyolite and metabasalt), older granitoids (grandiorite), (Fig. 76) and reworked hammamat sedimentary rocks. The crystal fragments are plagioclase, quartz, perthite, iron oxides, actinolite and chlorite, where these crystals are highly brecciated. The matrix is mainly composed of quartz, plagioclase, iron oxides with subordinate amount of actinolite. The quartz grains commonly show undulose extinction and are corroded by plagioclase, actinolite and iron oxides. Plagioclase shows the lamellar twinning feature. Actinolites are highly chloritized. Sometimes, the matrix contains fragments of fine quartz (Fig. 77).

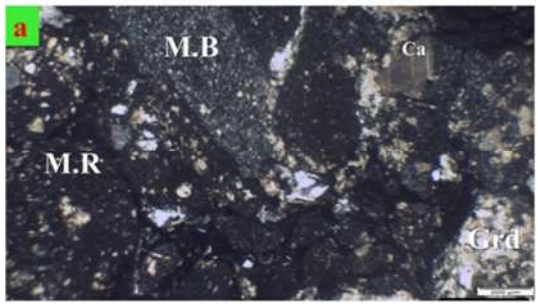

Fig. 76: Lithic fragments of metarhyolite (M.R), metabasalt (M.B) and granodiorite (Grd) in conglomerates.

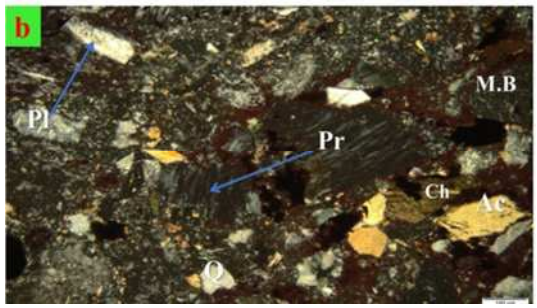

Fig. 77: Lithic fragments of metabasalt (M.B) with plagioclase (Pl), quartz (Q), perthite (Pr), actinolite (Ac) and chlorite (Ch) in conglomerates.

3.5.2 GREYWACKES

Greywackes are composed of crystals and rock fragments embedded in

fine to very fine groundmass with no definite orientation. The crystals are mainly represented by quartz and plagioclase, orthoclase, carbonates and chlorite. Quartz shows undulose extinction and sometimes shows amoeboid shape due to corrosion by the matrix constituents. Plagioclase crystals are usually altered until they lose their identity. The less altered crystals show lamellar twinning. Orthoclase crystals show their simple twinning feature and corrode in the carbonate and quartz crystals. The matrix is mainly composed of clay minerals and iron oxides with subordinate amounts of quartz, feldspars, micas, epidote and chlorite. Carbonates and iron oxides are disseminated all over the rock (Fig. 78). The rock fragments are represented by metarhyolite, metaandesite and metabasalt and corrode in each other and by quartz, they have small inclusions of iron oxides and plagioclase. The greywackes are highly cracked and cracks are filled with carbonates, clay minerals and iron oxides (Fig. 79).

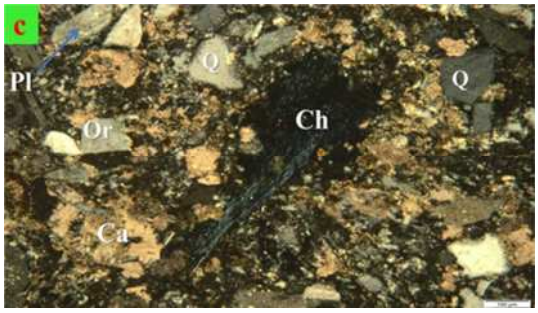

Fig. 78: Crystal fragments of quartz (Q), carbonate (Ca), chlorite (Ch), orthoclase (Or) and plagioclase (Pl) in greywacke.

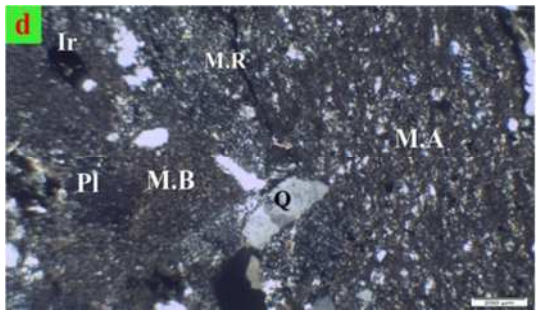

Fig. 79: Lithic fragments of metaandesite (M.A), metarhyolite (M.R) and metabasalt (M.B) with crystal fragments in greywacke.

3.5.3 PURPLE SLATES

Slates are characterized by its colour varying from purple to violet colour. They are very fine to fine grained, highly fissile and have well-developed slaty cleavages. Microscopically, these slates consist of quartz grains in silty and ash size (< 1/64 mm), muscovite, hematite and chlorite forming alternating light fine and dark very fine laminae. The light bands are mainly composed of detrital quartz of silt size having a reddish color in the polarized light. The dark laminae are composed of sericite, chlorite and hematite (Fig. 80). Generally the slates are invaded by calcite veinlet cutting all laminae (Fig. 81).

It is worth to mention that, the Hammamat sedimentary rocks have suffered from low- grade regional metamorphism where chlorite and epidote are present at the expense of other silicate minerals.

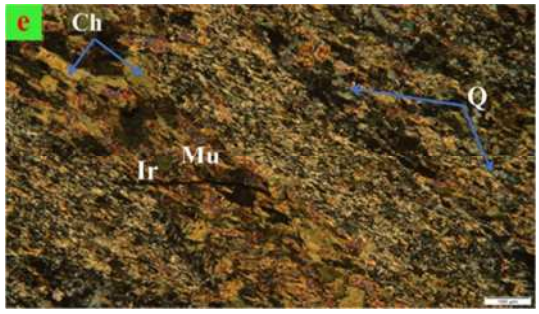

Fig. 80: Mutual laminaes of muscovite (Mu) and quartz (Q) with inclusions of chlorite (Ch) and iron oxides (Ir) in slates.

Fig. 81: Carbonate (Ca) veinlets within slates.

3.6 YOUNGER GRANITES

The younger granites in the study area could be classified into two phases; the first one is of greyish pink colour while the second phase is of red colour. Q-A-P triangle (Streckeisen, 1976) is used for the classification of the younger granites. In the present work, five thin sections were chosen for modal analyses. The results were tabulated in table (2). The greyish pink granites plot within the syenogranite field while the red granites plot within the alkali granite field (Fig. 82) due to very high content of potash feldspar in this phase of younger granites, accordingly this granite could be considered as alkali feldspar granite.

Table (2): The modal analyses of the studied younger granites of the area.

Rock type	S. No.	Mineral composition					
		Quartz (Q)	K-Feldspar (A)	Plagioclase (P)	Biotite	Acssessories & opaques	Total
Syeno-granite	47	28.20	44.70	20.57	4.10	2.43	100%
	48	31.61	43.65	18.02	4	2.72	100%
Alkali feldspar granite	50	41.40	54.66	1.60	1.40	0.94	100%
	51	45.20	48.70	1.90	2.10	2.10	100%
	52	43.51	50.70	1.59	1.80	2.40	100%

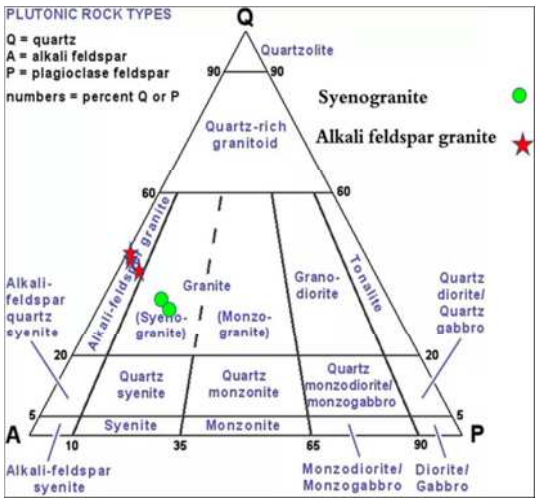

Fig. 82: Ternary diagram (Streckeisen, 1976) for modal quartz (Q), alkali feldspar (A) and plagioclase (P) of the studied younger granites.

3.6.1 SYENOGRANITES

These rocks are generally equigranular, medium to coarse-grained with hypidiomorphic and graphic textures. They are mainly composed of potash feldspars, quartz and biotite with subordinate amounts of plagioclase as essential minerals. Zircon and iron oxide are the main accessory minerals. Sericite, muscovite and epidote are found as secondary minerals. The presence of two feldspars phases (potash feldspars and plagioclase) suggests that these granites are mostly subsolvus and crystallized under high water vapour pressure (Greenberg, 1981).

Potash feldspars are the most dominant minerals in these rocks. They form 43.65% to 44.7 % of the modal composition (table 2). They are represented by microcline perthites. Microcline perthite occurs as subhedral to euhedral crystals ranging in size from 0.5 to 3.4 mm across.. They are often cracked; most of the cracks are filled with iron oxides, muscovite and epidote (Fig. 83). The microcline perthite is restricted to the syenogranite near the contact with alkali feldspar granite.

Quartz is less dominant than potash feldspars. It forms 28.2% to 31.61 % of the modal composition (table 2). It is found as medium to coarse anhedral crystals of various shapes ranging in size from 0.4 to 2.8 mm across (Figs. 84 and 86).

Plagioclase occurs as subhedral to euhedral albite-oligoclase (An_{5-20}) crystals ranging in size from 0.35 to 1.7 mm across. It forms 18.02% to 20.57 % of the modal composition (table 2). Plagioclase crystals are completely altered to sericite. These crystals show the antiperthite texture and are cracked (Fig. 85).

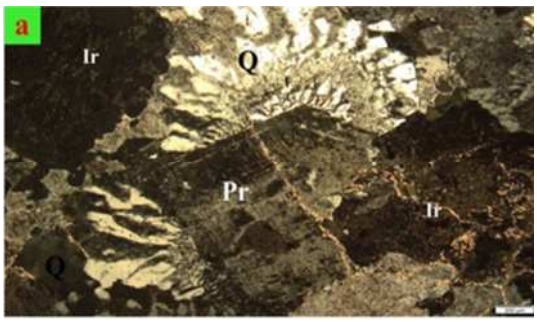

Fig. 83:The growing of quartz (Q) grains on the outer rims of the perthite (Pr) crystal showing the graphic texture with inclusions of iron oxides (Ir) in syenogranite.

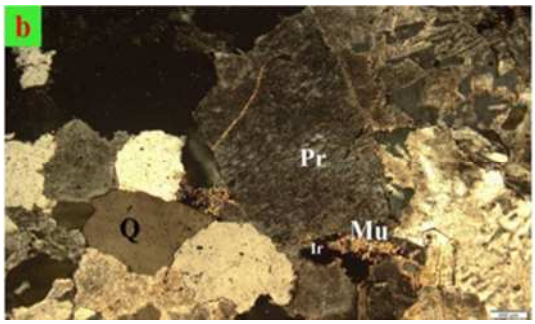

Fig. 84: The perthite crystal is fractured and corroded by the quartz (Q), muscovite (Mu) and iron oxides (Ir) in syenogranite.

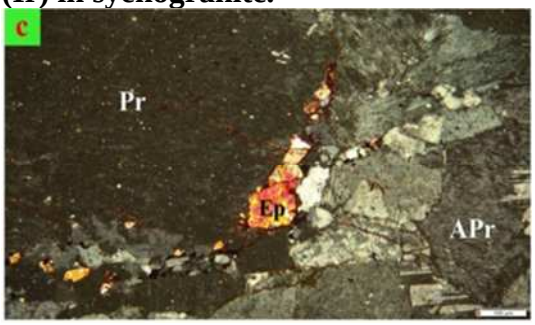

Fig. 85: perthite (Pr), antiperthite (APr) and epidote (Ep) in syenogranite.

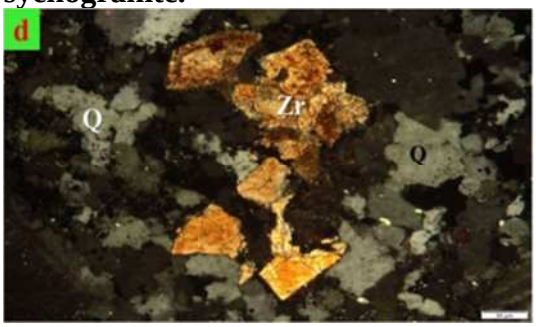

Fig. 86: Zircon (Zr) crystals corroded by quartz (Q) in syenogranite

3.6.2 ALKALI FELDSPAR GRANITES

Alkali feldspar granites are generally equigranular, medium to coarse-grained with hypidiomorphic texture. They are composed of potash feldspars, quartz, plagioclase, biotite and muscovite as essential minerals. The main accessory minerals are zircon, epidote and apatite while the main secondary minerals are iron oxides and muscovite. Some samples are mainly composed of potash feldspars and quartz

with very few or absence of plagioclase crystals, suggesting transsolvus to hypersolvus texture (Martin and Bonin, 1976).

Potash feldspars are fairly abundant. It forms 48.7% to 54.66 % of the modal composition (table 2). They are represented by orthoclase and microcline perthites, but microcline perthites are the predominant(Figs 87, 88 and 89).

Quartz is less dominant than potash feldspars where it forms 41.4% to 43.51% of the modal composition (table 2). It occurs as anhedral to subhedral crystals ranging in size from 0.3 to 2.9 mm across. Minute worm-like or finger-like bodies of quartz form the myrmekitic texture (Figs.87, 88 and 90).

Plagioclase occurs as subhedral prismatic crystals ranging in size from 0.4 to 3.4 mm across. It is composed of albite (An $_{5\text{-}10}$) and forms 1.6% to 1.9 % of the modal composition (table 2). They poikilitically enclose quartz and iron oxides, and have clear cracks which are filled with the secondary muscovite mineral (Fig. 89).

Biotite is present in minor amounts as flakes which are brown to yellowish brown in colour, pleochroic and mottled with iron oxides. They are corroded by quartz and perthite to different degrees until some islets are completely separated and surrounded by the other silicate minerals. Some biotite flakes poikilitically enclose iron oxides (Figs.87, 88 and 90).

Muscovite occurs as small anhedral flakes growing in the interstitial spaces between silicate minerals.. Also it is encountered as secondary mineral filling the cracks or replacing feldspars. Muscovite flakes are corroded by feldspars and quartz (Fig. 89).

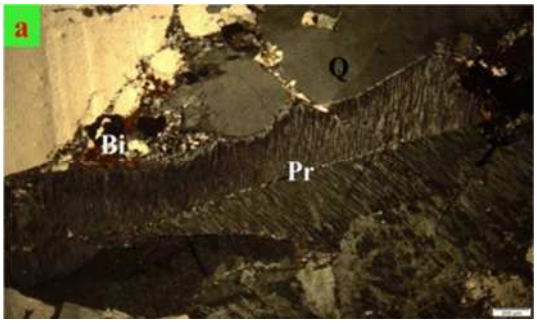

Fig. 87: The orthoclase perthite (Pr) corroded by the quartz (Q) and biotite (Bi) crystals in alkali feldspar granite.

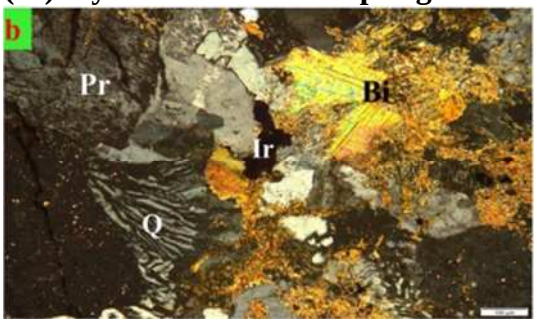

Fig. 88: Quartz (Q) with perthite (Pr) show the myrmikitic texture, iron oxides (Ir) and biotite (Bi) in alkali feldspar granite.

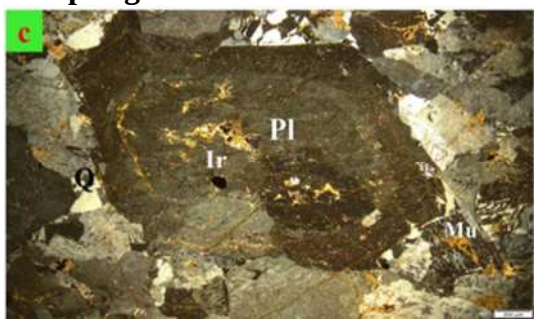

Fig. 89: Zoned plagioclase with inclusions of iron oxides (Ir), musconite (Mu) and quartz (Q) in alkali feldspar granite.

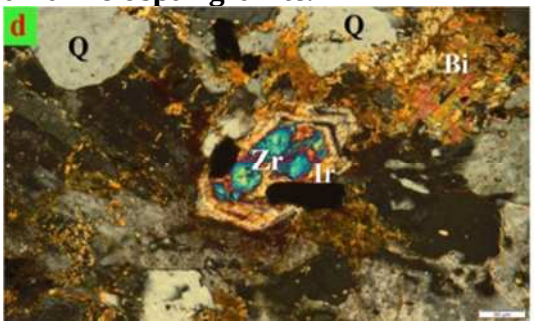

Fig. 90: Zircon (Zr) crystals corroded by quartz (Q), biotite (Bi) and iron oxides (Ir) in alkali feldspar granite.

From the previous characteristics, it could be concluded that the alkali feldspar granites has the same mineral composition and the same texture of the syenogranite with some differences which could be summarized as follows:

1- The potash feldspars of alkali feldspar granites are highly exceeding the plagioclase. In some samples, plagioclase become very rare or absent.

2- Microcline perthite in alkali feldspar granites is more dominant than orthoclase perthite. Biotite in alkali feldspar granites is found in large amounts.

3- Alkali feldspar granites, generally, show less deformation than the syenogranite. This could be interpreted by the less undulose extinction of quartz and less fracturing of feldspars.

3.7. POST GRANITE DYKES

They are classified into three groups: acidic, intermediate and basic dykes.

3.7.1. ACIDIC GRANOPHYRE DYKES

These rocks are hard, massive, fine grained and varying in colour from reddish pink, pink to red colour with smoky quartz grains and manganese dendritic shapes.

Microscopically, they are distinguished by graphic and granophyric textures. They are mainly composed of medium grained quartz, K-feldspars and plagioclase set in a fine grained granophyric, crystalline groundmass displaying micrographic texture. Biotite, muscovite, apatite, carbonates and opaques are accessories, whereas sericite, chlorite and clay minerals are secondary minerals (Figs.91 and 92).

3.7.2 BASIC DOLERITE (DIABASE) DYKES

Basic dykes are fine to very fine grained and melanocratic of grey colour with few white medium grained crystals.

They are medium to fine grained and melanocratic of greenish grey to grey colour. Microscopically, these rocks are characterized by doleritic texture (Fig. 93) and mainly composed of calcic plagioclase, clinopyroxene and hornblende. Apatite and opaques are the main accessory minerals. Chlorite, epidote and saussurite are secondary minerals as alteration products of mafics and feldspars (Figs.93 and 94).

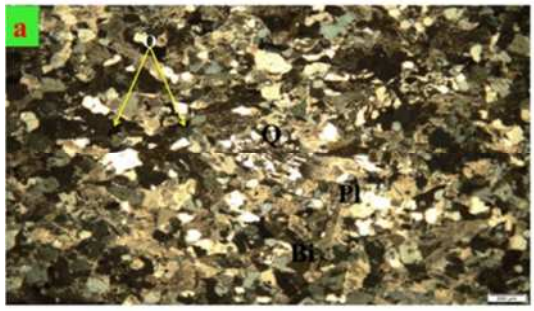

Fig. 91: Intergrowing crystals of quartz (q) and potashfeldspar showing graphic texture , biotite (bi), plagioclase (Pl) and opaques (O) in acidic granophyre dyke.

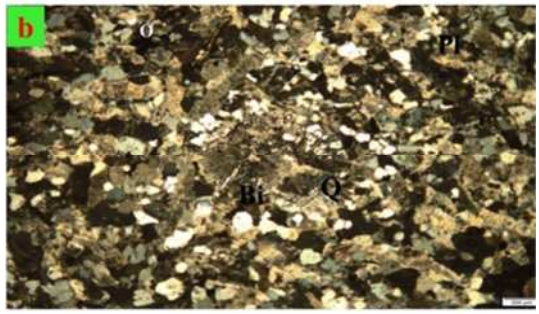

Fig. 92: Crystals of quartz (q) ,biotite (bi), plagioclase(Pl) and opaques (O) in acidic granophyre dyke.

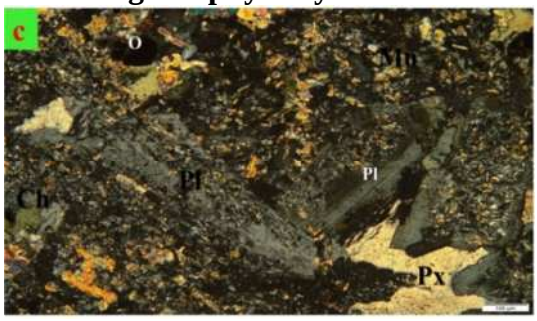

Fig. 93: Crystals of partially altered plagioclase (Pl), muscovite (Mu), pyroxene (Px) and opaques (O) in basic diabase dyke.

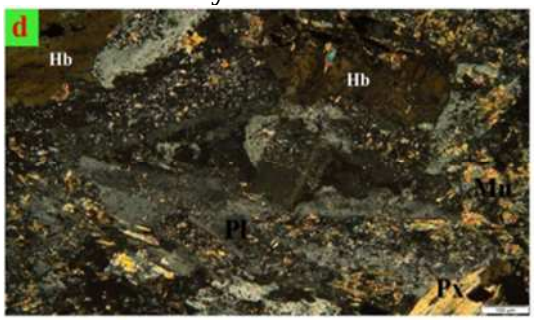

Fig. 94: Crystals of plagioclase(Pl), muscovite (Mu), pyroxene (Px) and hornblend (Hb) in basic diabase dyke.

III. RADIOACTIVITY

The emitted natural gamma radiation that transmitted from the rocks is a function of their radioelements content. These radioelements are Uranium, Thorium and Potassium (K_{40}), together with their decay series. Gamma rays are the most fundamental nuclear radiation, which detected because of its penetration ability in various media, as well as its long range. In the Uranium (U) and Thorium (Th) decay series, a number of intermediate isotopes are involved before reaching the steady point. In the Uranium series, the highest energy gamma ray emitter is Bi_{214} in the same time the strongest gamma emitter in the Thorium series is the Tl_{208}. For these radioelements detection, the measured intensity radiation principally resulted from these two isotopes. The concentration of Uranium and Thorium is proportional to the concentration of 214Bi and 208Tl, respectively, when reaching the state of stability and balance.

IV.1: Radioactivity of the Different Rock Unites

There is a general and marked relation between the age of the rock unit and its radioactivity from one side as well as the relation between the increase of the radioactivity and the increase of the acidity of the rocks (magmatic differentiation). This is to be expected because both U and Th are trace elements incompatible with the major rock-forming minerals. Hassan and Hale (1988) reached the same conclusion from their γ-spectrometric determination of eU, eTh and K in the uraniferous granites and rhyolites of Devonian-Carboniferous age in southern new Brunswick in Canada. So, Radiometric survey is conducted to this area due to the presence of abundant granitic rocks of different types, contacts with other older volcanic rocks and remarkable features of late magmatic pneumatolytic phase and post-magmatic hydrothermal products such as pegmatite and aplite formation and different wall rock alterations associated with these granites. The radioactivity of the different rock types cropping out in the area under consideration were measured for the equivalent uranium (eU) and equivalent thorium (eTh) in part per million (ppm) by using a portable gamma-ray spectrometer (RS-230). Results of the filed radiometric survey measurements and laboratory measurements of the

various rock types in the study area will be discussed in some details as following. Table (3) show the variation in radioactivity for the different rock units recorded in the study area in both the field measurements and radiometric lab analysis.

IV.1.1: METAVOLCANICS

These rocks are generally of low radioactivity values if compared with other rock types. This is due to the low concentration of the radioelements content as they are mostly derived from Island arc. The radioactivity values of these metamorphosed volcanics are ranging from 90-150 cps. while the laboratory measurements show U radioactivity values ranging from 309-710 cps and the U concentration measured is under the detection limits. The Th radioactivity measured is ranging from 534 – 1103 cps while the Th concentration is ranging 2- 11 ppm. K has laboratory radioactivity values ranging from 404-767 cps while its concentration is ranging 1.9 – 4.9%.

IV.1.2: META-GABBRO –DIORITE COMPLEX

There is a great similarity between the values of both field and laboratory measurements of metagabbro-diorite complex and the previously mentioned metavolcanics due to their same origin as these are plutonic and volcanic equivalents. The gabbros has 85-90 cps field radioactivity. While the U is still under the detection limit Th has values ranging 2-11 ppm.

IV.1.3: OLDER GRANITOIDS

The older granitoids have a field radioactivity ranging from 90-190 cps while the laboratory measurements of uranium concentration is still under the detection limits. The Th has a range from 6-13 ppm which is slightly higher than metagabbro. K% is ranging from 2.6 - 4.3 also higher than the metagabbros.

IV.1.4: Dokhan Volcanics

Radioactivity is a powerful tool to differentiate between metavolcanics and Dokhan volcanics when it is difficult to diagnose between them geologically. Field radioactivity for Dokhan volcanics is ranging from 110-150 cps while their U concentration is also under the detection limit. The thorium concentration in the laboratory samples ranges from 1- 9 ppm while the K% is ranging from 2.1-4.4%.

IV.1.5 : HAMMAMAT SEDIMENTS

These sediments has a field radioactivity ranging from 105- 130 cps while the U concentration is under the detection limit for the laboratory samples. The thorium concentration is ranging from 3-5 ppm whereas the K% is ranging from 1.8 - 1.9 %. The low values of radioelement concentration for these sediments is attributed to the diffecincy of U, Th and K in the source Areas from which they were derived.

IV.1.6 : YOUNGER GRANITES

The younger granitic rocks show the highest values of radioactivity and radioelements concentration among the other rocks of the study area. This is due to its high differentiation index which causes U and Th to be enriched in the magma from which they were crystalized. Their field measurements show a radioactivity ranging from 180 – 3000 cps. The U concentration is ranging from 1-115 ppm while Th is recorded to

reach up to 482 ppm and K% reaches up to 5.78 % for the anomalous pegmatite samples.

Table (3): Field and laboratory measurements of radioactive elements ; U, Th and Re (in C.P.S. and p.p.m) and K (in C.P.S. and%) in the different rock units of the studied area .

Rock unit	*Field measurement c.p.s*	(U) c.p.s	(U) p.p.m	(Th) c.p.s	(Th) p.p.m	(Re) c.p.s	(Re) p.p.m	(K) c.p.s	(K) %
Younger granites	3000	17839	115	25654	482	15611	141	2661	5.78
	3000	12655	71	19855	414	8944	42	1370	1.28
	230	664	6	992	12	761	6	677	5.04
	180	742	1	1095	13	785	4	670	4.03
	400	1054	4	1515	23	1101	9	698	4.64
	240	1481	5	2088	30	1622	17	771	4.7
	130	358	*Less than 5 P. P. m.*	570	5	524	5	352	1.8
Dokhan volcanics	110	365		557	1	532	3	564	3.9
	130	561		865	9	659	4	648	4.4
	150	543		796	7	694	5	447	2.1
Older granites	90	744		1188	13	836	4	745	4.3
	190	565		923	8	761	5	645	3.9
	100	434		714	6	645	6	454	2.6
Meta gabbros	85	477		752	10	599	5	457	3.1
	95	262		512	2	501	4	353	1.5
	90	380		588	3	580	5	437	2.6
Meta volcanics	130	710		1103	11	842	5	757	4.9
	90	625		920	10	781	6	414	1.7
	95	309		534	2	494	3	404	1.9
	100	479		807	8	646	4	523	2.9
	150	537		878	7	695	4	738	4.8

IV.2: RADIOACTIVE ANOMALY IN THE AREA

This anomaly is located at the northern flank of W. Ladid Al Jiudan in alkali feldspar granites. The high gamma-radioactivity is linked to a pegmatite vein of 1.3m width and can be traced clearly for 10 - 15meters length extending in nearly N-S direction (Fig. 95) . The granites surrounding the pegmatite vein are nearly nearly alterd with abundant hematitization and Mn-oxides and are cut by basic dykes, and veins of quartz with slight hematitic staining on the walls of joints. Radiometric contour map is made for the anomalous pegmatite in W. Ladid Al-Jui'dan (Fig. 96).

The radiometric field measurements of the anomalous zone indicate the presence of elongated and stretched high radioactive zone strongly controlled by the pegmatite vein. The background gamma radioactivity of the alkali feldspar granites near the radioactive anomaly is 350 cps, while the pegmatite vein has a gamma radioactivity up to 3000 cps (table 3). The laboratory measurements for the grab sample which collected from this anomalous zone indicate that the equivalent uranium content equal 115 ppm, while the eTh is 482 ppm which indicates a Thorium Anomaly controlled by these pegmatites.

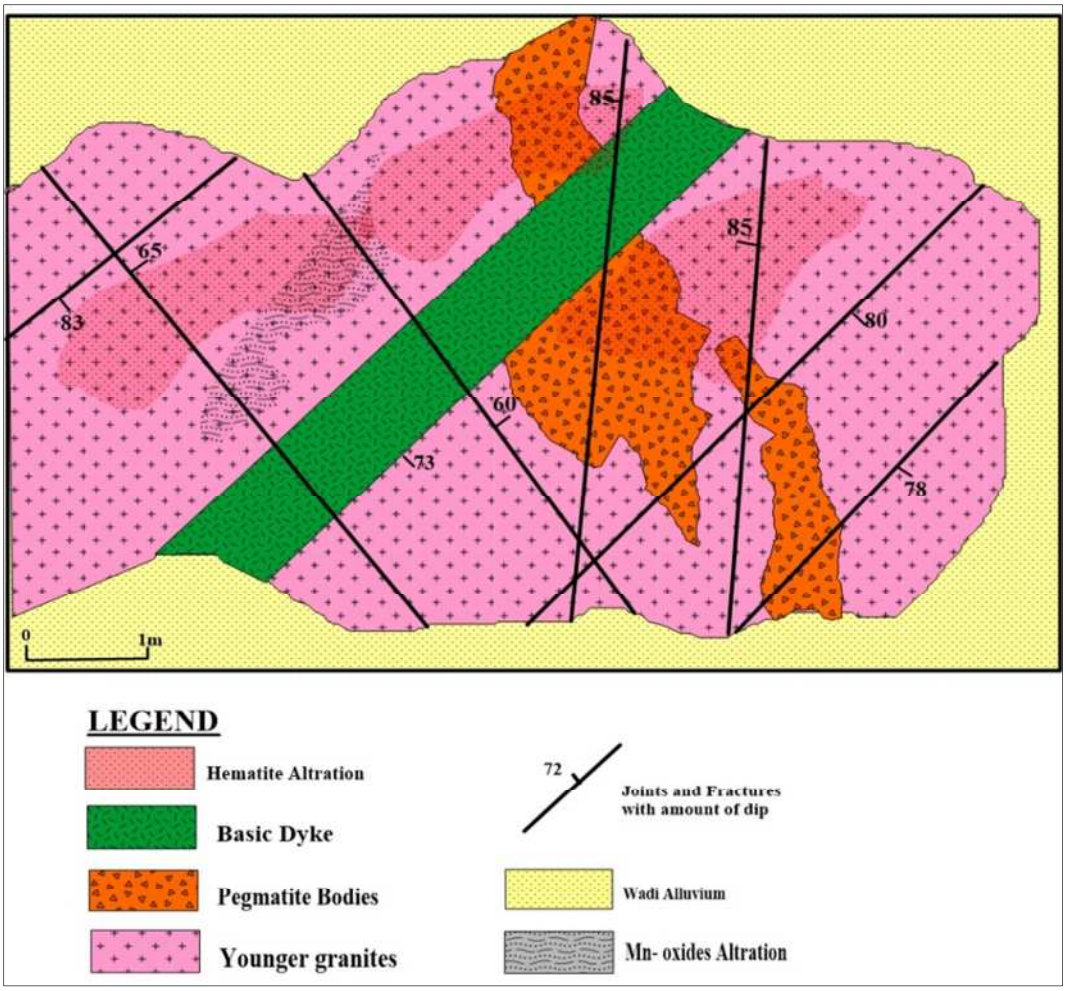

Fig. 95: To scale Sketch Map for the Anomalous zone of pegmatite in the Alkali feldspar granites along W. Ladid Al- Jui'dan.

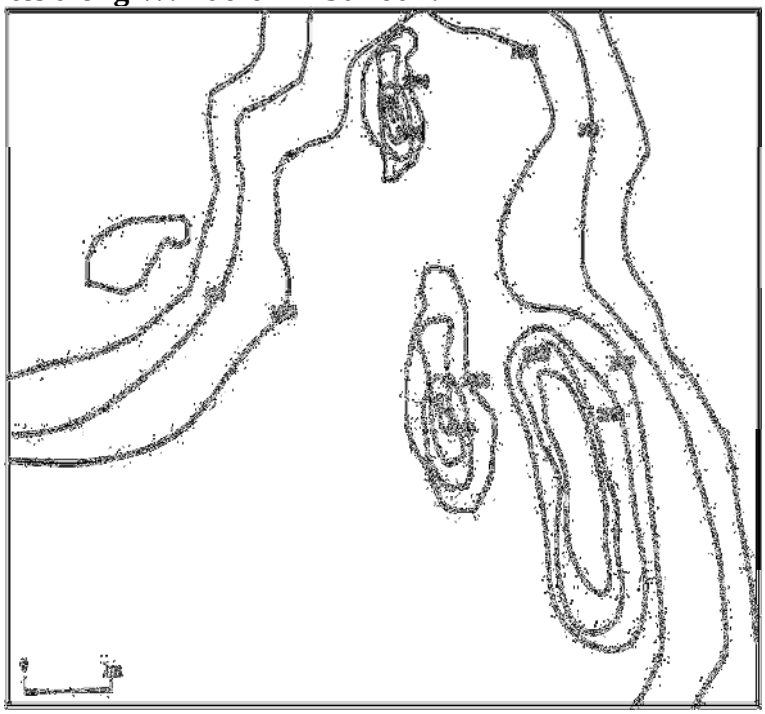

Fig. 96: Radiometric contour map for the anomalous pegmatite W. Ladid Al- Jui'dan**.**

V. CONCLUSION

A varieties of rocks including metavolcanics, metagabbro-diorite complex, older granitoids, Dokhan volcanics, Hammamat sediments, younger granites as well as dyke swarms and veins are well exposed and studied in details at the strip enclosed between Wadi (W) Dib and W. Mellaha area. The metavolcanics is represented by the basic variety of metabasalt, intermediate variety of meta-andesite and acidic varities of meta-dacite and meta-rhyolites in addition to meta-pyroclastics. The metagabbro-diorite complex is shown intruding the metavolcanics and enclave rafts of then while this complex is intruded by both the older and younger granites and maily have the composition of metamorphosed gabbros. The older granitoids in the area are seen extruded by the Dokhan volcanics and are intruded by the younger granites and mainly have the composition of quartz- diorite and granodiorites when plotted on Streckeisen, 1976.

The Dokhan volcanics in the study area are present and exposed at W. Dib, W. Abu Had and W. Mellaha while they are represented by successive sequences of lava flows ranging in composition from intermediate to acidic varieties with their related pyroclastics. A wide spectrum of different types of molasses rocks is represented by the Hammamat sediments which have conglomerates, greywakies and purple slate and siltstone. The younger granitic rocks which are considered the most important, from the radioactivity point of view, are classified into syeno-granite and alkali feldspar granite varieties Streckeisen, 1976**,** and are shown intruding all the rock units exposed in the area. Numerous post-granitic dyke swarms and veins are recorded as basic and acidic dykes invading and cutting all the rock types exposed in the area.

The radioactivity of the rocks in the study area show an increase in their values from the older unites to the younger one which radioactivity is in harmony with the increase of the radioelement content. The younger granitic rocks show the highest values of radioactivity among the other rock units. An anomalous pegmatite body is located along a tributary branched from W. Mellaha has 157 ppm uranium content and 4350 ppm thorium content and 4.23 K% and is formed at the pnumatulitic stage of the alkali feldspar granites so one can conclude that it is thorium bearing pegmatite rather than uranium bearing pegmatite.

IV. REFERENCES

Abu El-Ela, A.M., 1985. Geology of W. Mubarak district, Eastern Desert, Egypt. Ph.D. Thesis, Tanta University.

Ahmed, A. and Ali, S.F., 2003. Geochemistry and radioactivity of the granitic rocks of Abu Had-Hawashiya area, north Eastrern Desert, Egypt. Proceedings of the 5th Int. Conf., on the Geology of the Middle East, 20-21 Jan. 2003, Cairo, p. 127-137.

Ahmed, A.M., 1983. Some petrographical and geochemical studies of G. Abu Had volcanics, Northern Eastern Desert, Egypt. M. Sc. Thesis, Geol, Fac. Sci, Al Azhar University, Cairo, Egypt. 127p.

Akaad, M.K., and Noweir, A.M., 1969. Lithostratigraphy of the

Hammamat-Um Seleimat district, Eastern Desert, Egypt. Nature, V. 223, p. 284 - 285.

Ali, M.A., 2001. Geology and petrology of some granitic rocks in the northern part of the Eastern Desert of Egypt. Ph. D. Thesis, Al Azhar Univ., Egypt, 294 p.

Ayoub, R.R., 2003. Geology and radioactivity of Gabal Um Tweir area, North Eastern Desert, Egypt. Ph. D. Thesis, Cairo Univ., Egypt, 286 p.

El Gaby, S., 1983. Architecture of the Egyptian basement complex. Proc. 5th. International Conference of Basement Tectonics, Cairo, v. 5, pp. 1-8.

El Gaby, S., 2005. Integrated evolution and rock classification of the Pan-African belt in Egypt. 1st Sympo. on the classification of the basement complex of Egypt, P. 1-9.

El Gaby, S., El-Nady, O.M. and Khudeir, A., 1984. Tectonic evolution of the basement complex of CED of Egypt. Geol. Runds., V. 73: 1019-1036.

El-Gaby, S., List, F.K. and Tehrani, R., 1988. Geology, evolution and metallogenesis of the Pan African belt in Egypt. In El Gaby, S. and Greiling, R.O. (eds.). The Pan African belt of north east Africa and adjacent areas. Braun Schweig (Vieweg) p. 17 - 68 .

El-Ramly, M.F. and Akaad, M.K., 1960. The basement complex in the central Eastern Desert of Egypt between latitudes 24o 30` and 25o 40` N. Geol. Surv. Cairo, V. 8, 35 p.

El-Ramly, M.F., 1972. A new geological map for the basement rocks in the Eastern and south Western Desert of Egypt (scale 1: 1000,000). Ann. Geol. Sur. Egypt, V. II, p. 1 - 18.

El-Ramly, M.F., Hussein, A.A. and Francis, M.H., 1976. The ring complex of Wadi Dib, north Eastern Desert, Egypt: Abstracts of papers presented at the fourteenth annual meeting of the Geological Society of Egypt, Cairo, 21 p.

El-Shazly, E.M., 1964. On the classification of the Precambrian and other rocks of magmatic affiliation in Egypt. 22nd Int. Geol. Congr. Proc. Sect. 10, India, p. 88 - 101.

El-Sheshtawi, Y.A., El-Tokhi, M.M. and Ahmed, A.M., 1995. Petrogenesis of the Dokhan volcanics of Wadi Dib and Wadi Abu Had, Esh El Milahah, north Eastern Desert, Egypt. Ann. Geol. Surv. Egypt, V. 20, p. 163 - 184.

Francis, M.H., 1971. Geology of the basement complex in the north Eastern Desert between latitude 27o 30` and 28o 00` N. Internal report (27/17). Geol. Surv. Egypt.

Francis, M.H., 1972. Geology of the basement complex in the north Eastern Desert between latitude 27o 30` and 28o 00` N. Ann. Geol. Surv. Egypt, V. II, p. 161 - 180.

Garson, M.S. and Krs, M., 1976. Geophysical and geological evidence of the relationship of Red Sea transverse tectonics to ancient fractures. Bull. Geol. Soc. Am. V. 87, p. 169 - 181

Ghoneim, M.F., Hassan, A.M. and Abu Anbar, M.M., 1999. Post-Orogenic and Rift-related ring complexes in Egypt: Geochemical and isotopic 246 - 265.discrimination. GAW4, Int.Conf. On Geol. Of the Arab World, Cairo Univ., Egypt. p. 246 - 265.

Hammad, H. M., 2005. Petrology and uranium distribution in the Abu Had granitic pluton, north Eastern Desert, Egypt. Journal of the

Faculty of Education, vol. 30, p. 67-90.

Hammouda, N. S., 1998. Geochemical properties of some Egyptian granitic rocks in the northern part of the Eastern Desert of Egypt. Ph. D. Thesis, Cairo Univ., Cairo, Egypt. 255 p.

Hassan, H. H. and Hale, W. E.,1988. Uraniferous granite and rhyolite of Devonian-Carboniferous age in Southwestern New Brunswick, Canada. Uranium, Vol. 4, P. 245-259.

Hassan, M.A. and Hashad, A.H., 1990. Precambrian of Egypt. In: Said, R. (ed.). The geology of Egypt, Balkema, Rotterdam, p. 201 - 245.

Hassanen, M.A., Mohamed, F.H., Abdel Maguid, A.A., Schmidt, W. and Shalaby, M.H., 1997. Geochemistry and petrogenesis of the Cambrian ring complex: An example of alkaline magmatism at Wadi Dib, Eastern Desert, Egypt. Chem. Erde. 57, p. 63 - 89.

Heikal, M.A. and Ahmed, A.M., 1982. Late Precambrian volcanism in G. Abu Had, Eastern Desert, Egypt: Evidence for island-arc environment. Acta. Miner. Petr., Szeged, V. 26: 221-223.

Heikal, M.A. and Ahmed, A.M., 1983. Some aspects of ignimbritic rhyolites of G. Abu Had, Dokhan volcanic rocks, Eastern Desert, Egypt. Ann. Geol. Surv. Egypt. v. XIII: 169-184.

Hume, W.F., 1935. Geology of Egypt. V. 2 Part 2, Geol. Surv. Egypt, Government press, Cairo, p. 301 - 688.

Hussein, A.A., Ali, M.M., and El Ramly. M.F., 1982. A proposed new classification of the granites of Egypt. J. Volc. Geoth. Res. V. 14, p. 187 – 190.

Martin, R.F. and Bonin, B., 1976. Water and magma genesis-the association hypersolvus granite-subsolvus granite. Canadian Mineralogist, V. 14, p. 228 - 237.8.

Masoud, M.S., Abdel Mola, A.F., El Sherbeni, H.A., Makhlouf, A.A., Hamouda, E.M., Moussa, M.A. and Azzam, H.M., 1998. Geology of Wadi Abu Had area, north Eastern Desert of Egypt. Internal report, Geol. Surv. Egypt, 79 P.

Mussa, M.A. and Dardier, I., 1982. Structural analysis of some granitoid rocks in the north Eastern Desert of Egypt. Ann. Geol. Surv. Egypt. Vol. XII, p. 180-209.

Rabie, S.I, Hussein, A.H. and Samy, H.A., 1996. Distribution and interpretation of radioelements, Wadi Dib area, north Eastern Desert, Egypt. Proc. Egypt. Acad. Sci. V. 46, p. 469 - 502.

Rabie, S.I, Hussein, A.H. and Samy, H.A., 1994. Magnetic and radiometric trends associations and their relation to uranium remobilization in Gabal El Gedan, Eastern Desert of Egypt. JKAU: Earth Sci. V. 7, p. 1 - 26.

Ragab, A.I., 1987. On the petrogenesis of the Dokhan volcanics of the north Eastern Desert, Egypt. M.E.R.C. Ain Shams Univ. Earth Sci. V. 1, p. 151 – 158.

Ressetar, R. and Monrad, J.R., 1983. Chemical composition and tectonic setting of the Dokhan volcanic formation, Eastern Desert, Egypt. J. Afr. Earth. Sci. V. 1, No. 2, p. 103 - 112.

Ries, A.C.; Shackleton, R.M.; Graham, R.H. and Fitches, W.R., 1983. Pan-African structures, ophiolites and mélanges in the Eastern Desert of Egypt, a traverse at 26º N.J. Geol. Soci., London, v. 140, pp. 75-95.

Sabet, A.H., Abdel Maksoud, A.M., and Nabrovenkov, U.S., 1977. Geological setting and petrography of Wadi Dib Ring intrusion, North Eastern Desert, Egypt. Geol. Surv. Egypt, V. 21, P. 91-102

Serencsits, C.Mc C., Faul, H., Roland, K.A., El-Ramly, M.F. and Hussein, A.A., 1979. Alkaline ring complexes in Egypt: their ages and relationship to tectonic development of the Red Sea. Ann. Geol. Surv. Egypt, V. IX, p. 102 - 116.

Stern, R.J. and Hedge, C.E., 1985. Geochronologic and isotopic constraints on late Precambrian crustal evolution in the Eastern Desert of Egypt. Amer. J. Sci. V. 258, p. 97 - 127.

Streckeisen, A., 1976. To each plutonic rock its proper name. Earth Sci. Rev. V. 12, p. 1 - 33.

Takla, M.A., 2002. Classification and Characterization of the Shield Rocks of Egypt. 6th Int. Conf. on Geol. of the Arab-World, Cairo Univ., Egypt, Abst., P. 32

(الملخص العربي)

جيولوجية وبتروجرافية واشعاعية المنطقة مابين وادي الدب ووادي ملاحه، شمال الصحراء الشرقية- مصر

حسام أنور خميس، درويش محمد الخولي، خيري سعد ذكي و محمد محمود محمد سعيد

تنوعات من الصخور تشمل البركانيات المتحوله، معقد الميتاجابرو والدايورايت والجرانيتات القديمه وبركانيات جبل الدخان ورواسب مولاس مجموعة الحمامات وصخور الجرانيت الحديث بالإضافة الي اسراب السدود والقواطع وعروق مابعد الجرانيت تمت دراستها بالتفصيل في الحزام الواقع بين وادي الدب ووادي ملاحة بشمال الصحراء الشرقية. تمثل البركانيات المتحولة من النوع القاعدي بالبازلت المتحول، والنوع المتوسط بالأنديسايت المتحول وبالانواع الحامضية من الداسيت المتحول والريوليت المتحول بالإضافة إلى رواسب الفتاتيات البركانيه المتحولة. يظهر معقد الميتاجابرو والدايورايت متداخلا في صخور البركانيات المتحولة اخذا منها مكتنفات صخرية مختلفة الاحجام، بينما يتداخل في هذا المعقد ويخترقة صخور كلا من الجرانيتات القديمة والحديثة، ويتكون عامة من صخور الجابرو المتحول. ويمكن رؤية الجرانيتات القديمة في منطقة الدراسة وهي تُقطَع بصخور بركانيات جبل الدخان و صخور الجرانيت الحديث وهي تمثل عامة بالكوارتز- دايواريت والجرانودايورايت.

تظهر منكشفات بركانيات جبل الدخان في منطقة الدراسة في غرب وادي الدب، غرب جبل أبو حد، وغرب جبل ملاحة حيث تمثل بتسلسلات متتالية من تدفقات الصهاره البركانية التي تتراوح في تركيبها من الأنواع المتوسطة كالانديزايت إلى الحامضية مثل الداسايت والريولايت مع مجموعة من رواسب الفتاتيات البركانية المرتبطة بها. تتمثل مجموعة واسعة من أنواع صخور المولاس في رواسب مجموعة الحمامات التي تحتوي على الكونجلوميرات والحجر الرملي الجريواكي وألاردواز ألارجواني اللون وأيضا الحجر الغريني ذو الحبيبات الدقيقة. وتصنف الصخور الجرانيتية الحديثة والتي تعتبر الأكثر أهمية من وجهة نظر النشاط الإشعاعي إلى أنواع السيانو- جرانيت وجرانيت الفلسبار القلوي وتظهر متداخلة وقاطعة لجميع الوحدات الصخرية المنكشفة في المنطقة. تم تسجيل العديد من انواع أسراب السدود والقواطع وعروق ما بعد الجرانيت على أنها سدود قاعدية وحمضية تغزو وتقطع جميع أنواع الصخور المكشوفة في المنطقة.

أظهرت بيانات النشاط الإشعاعي للصخور في منطقة الدراسة زيادة في قيمها من الوحدات الأقدم إلى الوحدات الأحدث عمرا حيث يتوافق النشاط الإشعاعي مع زيادة محتوى العناصر المشعة. تُظهر الصخور الجرانيتية الحديثة قيمًا أعلى للنشاط الإشعاعي بين الوحدات الصخرية الأخرى. وتم تسجيل شاذه اشعاعية في احد أجسام وعروق البيجماتايت على طول امتداد رافد متفرع من وادي لديد الجعدان ويحتوي على ١٥٧ جزء في المليون من اليورانيوم و٤٣٥٠ جزء في المليون من الثوريوم و٤.٢٣ % من البوتاسيوم والذي تم تكوينه في المرحلة الاخيرة لجرانيت الفلسبار القلوي والتي تسمي مرحلة البجماتايت ومن هنا يمكن القول انها بجماتايت حاملة للثوريوم اكثر منها لليورانيوم.